Novel Er^{3+} Perfluorinated Complexes for Broadband Sensitized Near Infrared Emission

Angelo Monguzzi,*,† Riccardo Tubino,† Francesco Meinardi,† Alessio Orbelli Biroli,‡ Maddalena Pizzotti,‡ Francesco Demartin,§ Francesco Quochi,|| Fabrizio Cordella,⊥ and Maria Antonietta Loi⊥

Dipartimento di Scienza dei Materiali, Università Milano Bicocca, Via R. Cozzi 53, 20125 Milano, Italy, Dipartimento di Chimica Inorganica, Metallorganica e Analitica "Lamberto Malatesta", Unità di Ricerca dell'INSTM, Università degli Studi di Milano, Via G. Venezian 21, 20133 Milano, Italy, Dipartimento di Chimica Strutturale e Stereochimica Inorganica, Università degli Studi di Milano, Via G. Venezian 21, 20133 Milano, Italy, Dipartimento di Fisica, CNR-INFM Slacs, Università di Cagliari, S.P. Monserrato-Sestu Km 0, 700, 09042 Monserrato, Italy, and Zernike Institute for Advanced Materials, University of Groningen, Nijenborgh 4, 9747 AG Groningen, The Netherlands

Received September 9, 2008. Revised Manuscript Received November 6, 2008

The synthesis and characterization of novel fluorinated Er^{3+} complexes emitting at the telecommunications wavelengths are presented. These new knowledge-based materials have been designed and optimized on the basis of an extensive photophysical investigation on the processes controlling the overall quantum yield, namely (i) the energy transfer process from the light harvesting conjugated antenna to the emitting ion and (ii) the nonradiative quenching of the lanthanide emission. The study of their photophysical properties has been used for the assessment of their application as active materials in a new generation of low-cost, optical communication amplifiers, based on solution-processed planar waveguides pumped by light emitting diodes (LEDs). Suitable ligands possessing a high-absorption cross-section (where commercially available LEDs operate), good energy level matching those of the ion, and high solubility in fluorinated polymers have been developed.

Introduction

Near-infrared (NIR) light sources falling into the silica transparency windows are currently very widely used in the telecom technologies applications for fast signal transmission. Even though in long haul transmissions, silica-based technology is still unchallenged, applications on local area networks (LAN), data links and computer networks, consisting of complex high density circuitry, call for low-cost alternative solutions for the signal regeneration and distribution. Plastic optical fibers (POF) have recently received increasing attention because of their clear technical advantages over glass fibers, such as mechanical flexibility and a large core diameter that make them suitable for LAN applications.[1,2] Moreover, transmission losses in polymers can be minimized with typical loss values of about 0.01 dB/cm at 840 nm and about 0.1 dB/cm at 1550 nm.

In silica-based devices, the typical method to obtain NIR light at the wavelength of 1550 nm is to exploit the emission of Er^{3+} trivalent ions due to the $^4I_{13/2} - {}^4I_{15/2}$ 4f intrashell electronic transition. Obtaining erbium based emitters compatible with polymeric matrices is however still an open and challenging task because rare earth ions are insoluble in polymeric films. A possible solution, which is presently pursued, is to employ organolanthanide complexes enough soluble and compatible to be used as dopants of POFs. These materials have the following advantages: (i) they can be easily dispersed in polymeric matrices to very high concentrations (up to 1×10^{21} ions/cm^3) without clustering; (ii) silica based erbium-doped fiber amplifiers (EDFA) operate with high power pump lasers at 980 and 1480 nm. At these excitation wavelengths, excited-state absorption (ESA) is a factor strongly limiting the optical gain. Moreover, such pump lasers constitute a significant fraction of the cost of a planar amplifier. In organolanthanide complexes, the ion excitation process is completely different because of the emissive state of the metal is indirectly populated by resonant energy transfer (RET) from optically excited light harvesting ligands. The large cross-section of the ligands and their broadband absorption allow the pumping by a white light source as a lamp or by a commerical LED rather than by a laser.

The use of organolanthanide complexes based emissive materials allows to fabricate low threshold active devices for electro-optical applications; for instance efficient visible emitters based on Eu^{3+} and Tb^{3+} complexes have indeed been obtained. An efficient emission is more difficult to be reached for organolanthanide complexes based on NIR emitting ions (Er^{3+} or Yb^{3+} or Nd^{3+}) where strong non radiative deactiva-

---

* Corresponding author. E-mail: angelo.monguzzi@mater.unimib.it (A.M). Tel.: 39-0264485173. Fax: 39-0264485400.

† Università Milano Bicocca.

‡ Dipartimento di Chimica Inorganica, Metallorganica e Analitica "Lamberto Malatesta", Università degli Studi di Milano.

§ Dipartimento di Chimica Strutturale e Stereochimica Inorganica, Università degli Studi di Milano.

|| Università di Cagliari.

⊥ University of Groningen.

(1) Kuriki, K.; Nishihara, S.; Nishizawa, Y.; Tagaya, A.; Koike, Y.; Okamoto, Y. *J. Opt. Soc. Am., B* **2002**, *19*, 1844–1848.

(2) Kuriki, K.; Koike, Y.; Okamoto, Y. *Chem. Rev.* **2002**, *102*, 2347–2356.

10.1021/cm8024445 CCC: $40.75

tion processes take place due to the dipolar coupling between the electronic transitions of the metal ion and the vibrational overtones of O−H and/or C−H bonds of the ligands.[3] This coupling is so efficient that for these systems a typical value for the NIR photoluminescence decay time is around 1 μs (to be compared with the typical radiative lifetime of a few ms), with a corresponding reduction of the emission quantum yield (QY). Recent researches suggest that the reduction of vibrational energies of the environment surrounding the ions, such as the use of a fully halogenated ligand,[4−7] could significantly increase the NIR emission lifetime.[8,9] However, in the materials so far proposed the absorption of the organic antenna is appreciable only below 300 nm,[10] which makes indirect pumping of the ions by using broadband, commercially available LEDs difficult.

We have thus tried to introduce a significant improvement of the properties of organolanthanide complexes emitting in the NIR by pursuing the following strategy:

1. Design of light-harvesting organic antennas with efficient energy transfer to the rare earth ion combined with absorption in the region where commercially light-emitting diodes are available.

2. Achievement of a significant reduction of the nonradiative deactivation exerted by the inductive electromagnetic coupling with high-frequency vibrational modes, for instance, by introducing fluorinated ligands acting as antennas. We have thus investigated both theoretically and experimentally the relationship between the quenching rate and the distance of the lanthanide ion from the C−H oscillators in order to provide precise synthetic strategies for the preparation of ligands in order to obtain more efficient NIR emitters. To this end, we have used time-resolved emission spectroscopy techniques to evaluate the extent of the quenching.

3. Improvement, by choice of appropriate fluorinated ligands, of the solubility of the organolanthanide complexes in suitable polymers possessing low optical losses in the NIR spectral window. This will provide the possibility of fabricating blends in which an efficient IR light amplification could be achieved.

In this paper, we report the synthesis and the photochemical and structural characterization of two new Er^{3+} highly fluorinated complexes.

Experimental Section

General. All solvents were purchased anhydrous over molecular sieves by Fluka and used without any other purification, except CCl_4 (Sigma Aldrich), which was distilled over P_2O_5. $Er(OAc)_3\cdot nH_2O$ was purchased by Sigma Aldrich and dried in vacuum over P_2O_5 at 100 °C before used, tris(pentafluorophenyl)phosphine oxide was prepared starting from tris(pentafluorophenyl)phosphine (Fluka) as previous reported,[11] 1,1,1,5,5,5-hexafluoropentane-2,4-dione (Hacac-F_6) was purchased by Sigma Aldrich and 1,1,1,3,5,5,5-heptafluoropentane-2,4-dione (Hacac-F_7) by Apollo Scientific Ltd.,[12] both used as received. Glassware has been always flame-dried under vacuum before use. ^1H, ^{31}P, and ^{19}F NMR spectra were recorded with a Bruker Avance DRX 300 spectrometers in CD_2Cl_2 (Cambridge Isotope Laboratories, Inc.) as solvent. Elemental analyses were carried out with a Perkin-Elmer CHN 2400 instrument in the Analytical Laboratories of the Department of Inorganic Metallorganic and Analytical Chemistry of Milan University.

Photoluminescence Studies. Electronic absorption spectra of complex **1** and **2** in CCl_4 solution were recorded by a Varian Cary 50 Scan spectrophotometer. For NIR PL measurements, the complexes, dissolved in CCl_4, were excited by a 355 nm (3.49 eV) Nd:YAG laser (Laser Export mod. LCS-DTL-374QT) with excitation power of 2.7 mW and a pulse repetition rate of 10 kHz. NIR luminescence spectra were detected by nitrogen cooled PMT (Hamamatsu R5509−73) with an high speed amplifier (Hamamatsu C5594) and a 74100 Cornestone 2601/4 (ORIEL) monochromator (bandpass 15 nm). For time-resolved measurements, a PCI plug-in multichannel scaler ORTEC 9353 was used in photon counting acquisition mode, with an overall time resolution better than 100 ns. Alternatively, VIS and IR spectra were excited by the second harmonic of a Ti:Sapph laser (Coherent MIRA 900), delivering a train of ~100 fs-long pulses at a repetition rate of 80 MHz at 365 nm. In this excitation setup, IR spectra were spectrally dispersed by an imaging polychromator (Optics Spec. 250is) coupled to a thermo-cooled InGaAs diode array (Andor iDus DU490A-1.7), while visible emission (recorded by an Hamamatsu EM-CCD digital camera C9100−13) was spectrally and temporally dispersed by an imaging polychromator coupled to a 2D-streak camera (Hamamatsu C5680 equipped with N5716−03 tube (VIS) and N5716−02 tube (IR)). In photoluminescence excitation experiments, excitation was provided by the output of a 1-kHz tunable laser delivering 200-fs-long pulses (TOPAS, Light Conversion), pumped by a Ti:Sapphire regenerative amplifier (Integra -I, Quantronix).

X-ray Structure Determination. a summary of the crystal data and refinement details for compounds **1**, **2** is given in Table 1. Intensity data were collected at room temperature on a Bruker Apex II CCD diffractometer using graphite-monochromatized Mo Kα radiation ($\lambda = 0.71073$ Å). Data sets were corrected for Lorentz-polarization effects and for absorption (SADABS).[13] All structures were solved by direct methods (SIR-97) and completed by iterative cycles of full-matrix least-squares refinement on F_o^2 and ΔF

---

(3) Artizzu, F.; Marchiò, L.; Mercuri, M. L.; Pilia, L.; Serpe, A.; Quochi, F.; Orrù, R.; Cordella, F.; Mura, A.; Bongiovanni, G.; Deplano, P. *Adv. Funct. Mater.* **2007**, *17*, 2365–2376.

(4) Van Deun, R.; Fias, P.; Diesen, K.; Binnemans, K.; Görller-Walrand, C. *Phys. Chem. Chem. Phys.* **2003**, *5*, 2754–2757.

(5) Van Deun, R.; Fias, P.; Nockemann, P.; Shepers, A.; Parac-Vogt, T. N.; Van Hecke, K.; Van Meervelt, L.; Binnemans, K. *Inorg. Chem.* **2004**, *43*, 8461–8469.

(6) Mancino, G.; Ferguson, A. J.; Beeby, A.; Long, N. J.; Jones, T. S. *J. Am. Chem. Soc.* **2005**, *127*, 524–525.

(7) Quochi, F.; Orrù, R.; Cordella, F.; Mura, A.; Bongiovanni, G.; Artizzu, F.; Deplano, P.; Mercuri, M. L.; Pilia, L.; Serpe, A. *J. Appl. Phys.,* **2006**, *99*, 053520(1−4).

(8) Van Deun, R.; Nockemann, P.; Gorller-Walrand, C.; Binnemans, K. *Chem. Phys. Lett.* **2004**, *397*, 447–450.

(9) Tan, R. H. C.; Pearson, J. M.; Zheng, Y.; Wyatt, P. B.; Gillin, W. P. *Appl. Phys. Lett.,* **2008**, *92* (1−3), 103303.

(10) Glover, P. V.; Basset, A. P.; Nockemann, P.; Kariuki, B. M.; Van Deun, R.; Pikramenou, Z. *Chem.—Eur. J.* **2007**, 6308–6320.

(11) Wall, L. A.; Donadio, R. E.; Pummer, W. J. *J. Am. Chem. Soc.* **1960**, *82*, 4846–4848.

(12) ^1H and ^{19}F NMR spectra evidence that the commercial 1,1,1,3,5,5,5-heptafluoropentane-2,4-dione does not show the 97% purity declared by Apollo Scientific Ltd. In particular, the presence of the CF_2H group is confirmed by both ^1H and ^{19}F NMR spectra with signals at 5.6 ppm (doublet) and at−76 ppm (doublet), respectively. The CF_2H group has a ratio of about 1:6 in comparison with CF_3 groups. Attempts to separate 1,1,1,3,5,5,5-heptafluoropentane-2,4-dione from 1,1,3,5,5,5-hexafluoropentane-2,4-dione by different chromatographic techniques failed, as the properties of the two compounds were too close.

(13) *SADABS Area-Detector Absorption Correction Program*; Bruker AXS: Madison, WI, 2000.

Table 1. Crystallographic Data and Structure Refinement Details

	1	**2**
formula	$C_{51}H_3ErF_{48}O_8P_2 \cdot CH_2Cl_2$	$C_{51}ErF_{51}O_8P_2 \cdot CH_2Cl_2$
cryst syst	monoclinic	triclinic
space group	$C2/c$ (No. 15)	$P\bar{1}$ (No. 1)
M.W.	1927.20	1981.17
a (Å)	44.518(4)	11.8578(8)
b (Å)	11.881(1)	12.7659(8)
c (Å)	23.881(2)	43.755(3)
α (deg)	90	90.06(1)
β (deg)	91.27(1)	97.61(1)
γ (deg)	90	110.18(1)
V (Å^3)	12628(2)	6154.2(7)
Z	8	4
T (K)	294(2)	294(2)
D_c (g cm^{-3})	2.027	2.138
μ (mm^{-1})	1.617	1.669
no. of measured reflns	58334	51158
no. of unique reflns, R_{int}	16418, 0.101	30030, 0.0301
no. of obsd reflns [$I > 2\sigma(I)$]	8738	23693
absorp corr	SADABS	SADABS
T_{min}, T_{max}	0.586, 1.000	0.791, 1.000
R	0.0584	0.0721
wR_2 [all data]	0.1709	0.1882

synthesis using the SHELXL-97 program (WinGX suite).[14-16] Hydrogen atoms, located on the ΔF maps, with the exception of those of the clathrated solvent molecules, were allowed to ride on their carbon atoms.

Crystallographic data for compounds **1** and **2** (excluding structure factors) have been deposited with the Cambridge Crystallographic Data Centre as supplementary publications CCDC-692813 and CCDC-692814. These data can be obtained free of charge via email or from CCDC, 12 Union Road, Cambridge CB2 1EZ, UK; fax: +44 1223 336033; e-mail: deposit@ccdc.cam.ac.uk.

Synthesis of [Er(acac-F$_6$)$_3$(OP(C$_6$F$_5$)$_3$)$_2$] (1). In a Schlenk tube under nitrogen atmosphere, Hacac-F$_6$ (154 mg, 0.740 mmol, 3 equiv) was added to a stirred mixture of Er(OAc)$_3$ (85 mg, 0.247 mmol, 1 equiv) and OP(C$_6$F$_5$)$_3$ (284 mg, 0.518 mmol, 2.1 equiv) in CH$_2$Cl$_2$ (10 mL). The mixture was heated at reflux for 1 h and then filtered under nitrogen. To obtain suitable crystals for X-ray determination, *n*-hexane (30 mL) was slowly added to obtain a double layer. In a few days, the mixture afforded pink crystals of X-ray quality. The crystals were collected on Buchner funnel, 144 mg were obtained (yield 31%). ^{19}F NMR (300 MHz, CD$_2$Cl$_2$, δ): −93.6 (CF$_3$), −140.3 (*p*-C$_5$F$_6$), −156.4 (*m*-C$_5$F$_6$). Anal. Calcd for $C_{51}H_3ErF_{48}O_8P_2$: C, 32.50; H, 0.16. Found: C, 32.26; H, 0.19.

Synthesis of [Er(acac-F$_7$)$_3$(OP(C$_6$F$_5$)$_3$)$_2$] (2). As in the experimental procedure described above Hacac-F$_7$ (343 mg, 1.517 mmol, 3 equiv) was added to a stirred mixture of Er(OAc)$_3$ (174 mg, 0.505 mmol, 1 equiv) and OP(C$_6$F$_5$)$_3$ (584 mg, 1.065 mmol, 2.1 equiv) in CH$_2$Cl$_2$ (20 mL). The mixture was heated at reflux for 1 h and then was filtered under nitrogen. Slowly n-hexane (60 mL) was added until to obtain a double layer. In a few days pink crystals of X-ray quality afforded. The crystals were collected on Buchner funnel and sublimated in vacuum (1 × 10^{-5} torr at 300 °C) in 30 min. Finally the sublimated powder was dried in a vacuum over P$_2$O$_5$ at 100 °C for 1 day. 416 mg were obtained (yield 42%). ^{19}F NMR (300 MHz, CD$_2$Cl$_2$, δ): −90.38 (s, CF$_3$), −139.61 (m, p-C$_5$F$_6$), −156.01 (m, m-C$_5$F$_6$). Anal. Calcd for $C_{51}ErF_{51}O_8P_2$: C, 31.60. Found: C, 31.46. The analytical determination of the amount of hydrogen could not give reliable values because the calculated amount for the presence of CF$_2$H groups per mole was too low (0.05%).

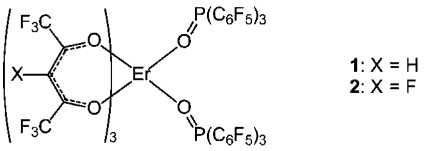

Figure 1. [Er(acac-F$_6$)$_3$(OP(C$_6$F$_5$)$_3$)$_2$] (**1**) and [Er(acac-F$_7$)$_3$(OP(C$_6$F$_5$)$_3$)$_2$] (**2**).

Results and Discussion

Design, Synthesis, and Structural Characterization. In addition to the features above-reported with respect to energy transfer processes and minimization of nonradiative deactivation, the Er^{3+} environment in an organolanthanide complex containing an organic antenna as ligand must also fulfill some other requirements, such as high thermodynamic and chemical stability, kinetic inertness, and a saturated coordination sphere.

To satisfy all these requirements, we have designed and synthesized the new Er^{3+} complexes reported in Figure 1, with a coordination sphere based on three partially (acac-F$_6$) or totally (acac-F$_7$) fluorinated chelating acetylacetonates and two triphenylphosphine oxides completely fluorinated ligands. The two fluorinated triphenylphosphine oxide ligands that complete the coordination sphere could act also as antennas, leading to highly NIR luminescent octa-coordinated complexes.

Complex **1**, with a coordination sphere based on three hexafluoroacetylacetonate (acac-F$_6$) ligands and complex **2** based on three heptafluoroacetylacetonate (acac-F$_7$) have been synthesized following a procedure reported for the synthesis of analogous Eu^{3+}, but without fluorinated triphenylphosphine oxide as ligands.[17] The synthesis was carried out in rigorously anhydrous conditions under a nitrogen atmosphere by reaction of the commercially available Er(OAc)$_3$ with OP(C$_6$F$_5$)$_3$ in anhydrous CH$_2$Cl$_2$. Slow precipitation by addition to the reaction solution of anhydrous n-hexane, yields pink crystals suitable for X-ray characterization. Selected crystal data and details of the crystal structure determination are reported in Table 1. Obviously, the X-ray characterization is unable to differentiate CF$_2$H and CF$_3$ groups.[12]

The X-ray structure determinations of complexes **1** and **2**, reported in Figures 2 and 3, shows that the Er^{3+} ion is in a square antiprismatic 8-fold coordination, surrounded by six oxygen atoms of three bidentate (acac-F$_6$) or (acac-F$_7$) ligands and by the oxygens of two fluorinated triphenylphosphine oxide ligands; the average Er−O distance is 2.323(4) Å, for both complexes.

The asymmetric unit of the crystalline network of complex **2** contains two independent molecules of the complex, slightly different in some conformational parameters. Moreover, at least one-half dichloromethane molecule is trapped in the crystalline structure of both compounds. The arrange-

---

(14) Altomare, A.; Burla, M. C.; Camalli, M.; Cascarano, G. L.; Giacovazzo, C.; Guagliardi, A.; Moliterni, A. G. G.; Polidori, G.; Spagna, R. *J. Appl. Crystallogr.* **1999**, *32*, 115–119.

(15) Sheldrick, G. M. *SHELX97−Programs for Crystal Structure Analysis (Release 97−2)*; University of Göttingen: Göttingen, Germany, 1998.

(16) Farrugia, L. J. *J. Appl. Crystallogr.* **1999**, *32*, 837–838.

(17) Petrov, V. A.; Marshall, W. J.; Grushin, V. V. *Chem Commun.* **2002**, 520–521.

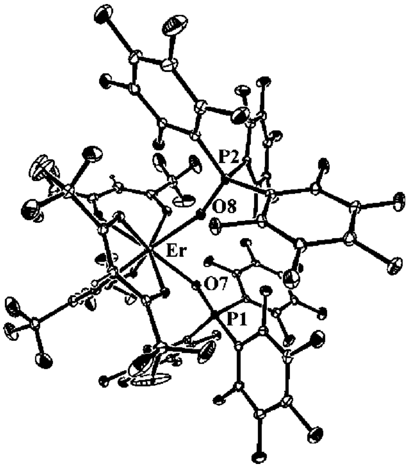

Figure 2. ORTEP view of the [Er(acac-F$_6$)$_3$(OP(C$_6$F$_5$)$_3$)$_2$] molecule of compound **1**.

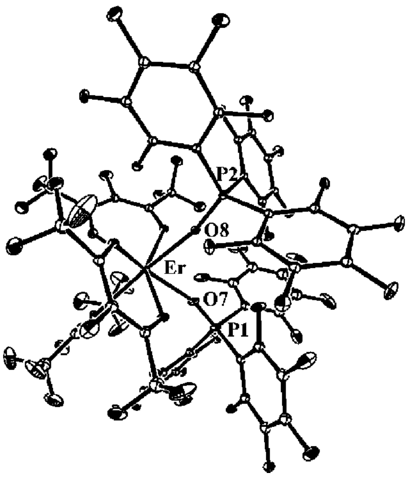

Figure 3. ORTEP view of one of the two [Er(acac-F$_7$)$_3$(OP(C$_6$F$_5$)$_3$)$_2$] independent molecules in the asymmetric unit of compound **2**.

ment of the fluorinated triphenylphosphine oxide ligands around the lanthanide ion is different from that reported by Petrov et al. for analogous Eu^{3+} complexes where two nonfluorinated triphenylphosphine oxide complexes are arranged trans to each other.[17] In the structure of both **1** and **2** the oxygen atoms of the fluorinated triphenylphosphine oxide ligands belong to the different square faces of the antiprism but display a cis arrangement with a O−Er−O angle of 80.9(2)° in complex **1**, 83.8(2) and 83.4(2)° in the two independent molecules of complex **2**, respectively. The O−Er−O angles involving the (acac-F$_6$) ligands range from 72.7(2) to 73.5(2)° in **1** and those involving the (acac-F$_7$) ligands range from 71.0(2) to 73.9(2)° in **2**. The central (O)C−C(X)−C(O) angles are more obtuse in **2** [X = F; average 124.1(9)°] than in **1** [X = H; average 121.3(7)°] because of the electron-withdrawing effect of the fluorine atom.

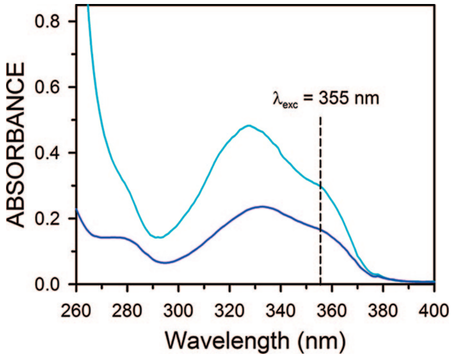

Figure 4. UV−vis absorption spectrum and NIR PL spectrum of complex **1** (sky blue line) and complex **2** (blue line) in CCl$_4$ solution.

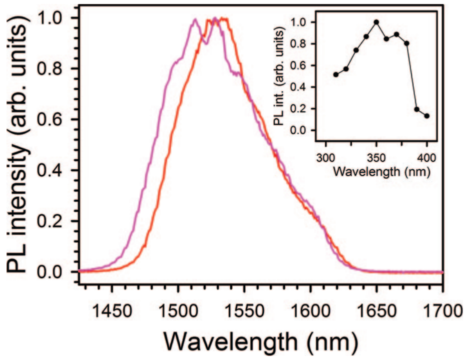

Figure 5. Normalized NIR PL spectrum of complex **1** (pink line) and complex **2** (red line) in CCl$_4$ solution. The inset shows the excitation profile at 1540 nm of complex **2** powder sample.

Compound **2**, after crystallization by CH$_2$Cl$_2$/*n*-hexane, has also been sublimed more than one time in order to guarantee the absence of solvent traces in the coordination sphere as required by efficient NIR photoluminescent properties. ^{19}F NMR spectra of compounds **1** and **2** are, as expected, very similar showing three signals at around −90 ppm (quite narrow) due to the CF$_3$ group, −140 and −156 ppm (broad) due to *para*- and *meta*-fluorine atoms of the triphenylphosphine oxide ligands. The signal of the fluorine atoms in ortho position of the fluorinated triphenylphosphine oxide and that bound to the central C atom of the acetylacetone ligand, which are close to the paramagnetic Er^{3+} ion, are too broad to be observed. Also, ^{31}P NMR spectra do not show any signal because of the closeness of phosphorus atom to the paramagnetic Er^{3+} ion.

Emission Lifetime Measurements. In Figure 4 are reported the electronic absorption spectra of complexes **1** and **2** in anhydrous CCl$_4$ solution (1.1 × 10^{-5} M for **1** and 1.8 × 10^{-5} M for **2**). Each complex shows a broad absorption band centered at 330 nm with a tail extending to 375 nm due to the aromatic fluorinated rings of the phosphine oxide ligands. No absorption lines of Er^{3+} ion are detected in the spectrum due to the low concentration of solutions.[18] Figure 5 shows their NIR PL under excitation at 355 nm: the emission peak centered at 1535 nm has the typical shape of Er^{3+} emission due to the $^4I_{13/2} - {}^4I_{15/2}$ electronic transition. The inset shows the excitation spectrum of the NIR emission (taken at 1540 nm) of complex **2** in polycrystalline powder. Photoluminescence excitation experiments were restricted to solid-state samples, as complexes in solution were found to be rather unstable when excited by ultrafast lasers. The broad sensitization profile reproduces the complex absorption band, indicating that energy is transferred to the Er^{3+} ion by RET from the fluorinated phosphine oxide acting as antenna. The excitation maximum is red-shifted with respect to the

---

(18) Lira, A. C.; Flores, M.; Arroyo, R.; Caldiño, U. *Opt. Mater.* **2006**, *28*, 1171–1177.

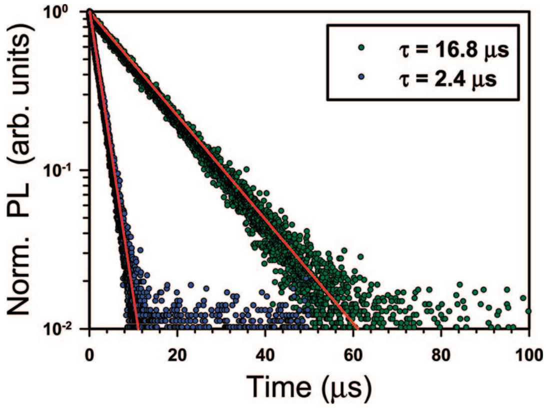

Figure 6. NIR PL decay at 1550 nm of complex **2** (green circles) and of complex **1** (blue circles) in CCl_4 solution ($\lambda_{exc} = 355$ nm). Red solid lines are the fit of data with a single exponential decay curve.

absorption maximum in solution because of aggregation effects, as already observed in other complexes.[3]

In Figure 6 are reported the decay curves for the NIR PL of **1** and **2** recorded at 1535 nm. Both curves are fitted well by a single exponential decay curve, which demonstrates the existence of a single emitting species for each sample and the lack of any energetic disorder. For complex **1** the lifetime of NIR luminescence is about 2.4 μs, whereas the lifetime of complex **2** is 1 order of magnitude higher with a value of 16.8 μs. The same behavior and values are obtained working on solid samples or at 77 K.

For each complex the PL lifetime (τ) is much shorter than the intrinsic radiative lifetime of Er^{3+} $^4I_{13/2}$ excited state (τ_{RAD}), which is about 10 ms in inorganic matrix.[19] By considering that the QY of PL ϕ is given by

$$\phi = \frac{\tau}{\tau_{rad}} \tag{1}$$

this implies that ϕ increases of 1 order of magnitude from about 2.4×10^{-4} (**1**) to 1.7×10^{-3} (**2**). This remarkable difference could be explained by considering the molecular structure of the two complexes. It is well-known that the Er^{3+} infrared emission is strongly quenched by the coupling with the vibrational energy levels of O−H or C−H bonds possibly present in the coordination sphere, whose overtones are resonant with ion emission energy. This electronic/vibrational coupling can be modeled by using the Förster theory on the energy transfer for dipole−dipole interactions.[20] By using this model it is possible to estimate the efficiency of the energy transfer from the donor D (the Er^{3+} ions) to the acceptor A (in the case of **1**, the C−H bond). The rate k_{DA} of the transfer could be computed by the following equation

$$k_{DA}(R_F) = \frac{g_i}{\tau_{rad}^{D}}\left(\frac{R_F}{|X_{DA_i}|}\right)^6 \tag{2}$$

where X_{DA_i} is the distance between donor and acceptor A_i, τ_{rad}^{D} is the radiative lifetime of donor, g_i is the multiplicity of A_i, and R_F is the Förster radius. R_F is a characteristic parameter of each donor−acceptor system and it depends on the transition dipoles and on the spectral overlap between donor emission and acceptor absorption

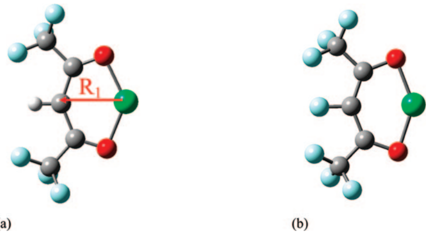

Figure 7. Detail of the chelating acac structure in complexes (a) **1** and (b) **2**.

$$R_F = 0.21[\theta^2 n^{-4} Q_D J(\lambda)]^{1/6} \tag{3}$$

where n is the refraction index of the material, θ is the factor which consider the reciprocal spatial orientation of the dipole moments involved in the transfer, Q_D is the donor emission QY, and $J(\lambda)$ is the integral overlap between D emission spectrum and A absorption.[21,22] If one assumes that the RET toward C−H (acting as acceptor) overtones is the dominant non radiative quenching mechanism we have

$$k_{DA}(R_F) = \frac{1}{\tau_{NR}} \tag{4}$$

and remembering that

$$\frac{1}{\tau} = \frac{1}{\tau_{RAD}} + \frac{1}{\tau_{NR}} \approx \frac{1}{\tau_{NR}} \tag{5}$$

when $\tau_{RAD} \gg \tau_{NR}$, it is possible to make a direct comparison between the k_{DA} computed by eq 2 and the overall decay time measured.

Figure 7 shows the structural detail of the location with respect the Er^{3+} ion of C−H bond of the acetylacetonate chelating ligand in complex **1.** The decay time of NIR emission can be accounted by considering the spatial distribution of the acceptor C−H bonds so that their contribution to NIR PL quenching can be evaluated by using eqs 2 and 3. For an oscillator strength of the C−H vibrational overtone of $f = 7.4 \times 10^{-8}$, we computed from experimental data a Förster radius $R_F = 9.6$ Å. We estimated the intrinsic radiative lifetime of the ion excited-state for both complexes by applying the Strickler−Berg formula on NIR absorption measurements; this lifetime, $\tau_{RAD} \approx 4 \times 10^{-3}$ s, and the distance of vibrational C−H groups from the heavy atom, $R_1 = 3.4$ Å, allows us to calculate the donor-to-acceptor transfer rate of complex **1**, $k_{DA} = 3.7 \times 10^5$ Hz, corresponding to a lifetime $\tau = 2.7$ μs.[21] Indeed, the measured lifetime τ is in very good agreement with the value estimated for the presence of three C−H bonds in the first coordination sphere and therefore it confirms our model as a suitable approach. In principle, complex **2** should possess a decay time comparable with the radiative lifetime of Er^{3+}, whereas the measured lifetime is only 1 order of magnitude higher than that of complex **1**. The reason for this discrepancy must be ascribed to the relatively low purity of the commercial Hacac-

---

(19) Zheng, Z.; Liang, H.; Ming, H.; Zhang, Q.; Xie, J. *Opt. Commun.* **2004**, *233*, 149–153.

(20) Förster, Th. *Ann. Physik* **1948**, *2*, 55–75.

(21) Ermolaev, V. L.; Sveshnikova, E. B. *Russ. Chem. Rev.* **1994**, *63*, 905–922.

(22) Howard, D. L.; Kjaergaard, H. G. *J. Chem. Phys.* **2004**, *121*, 136–140.

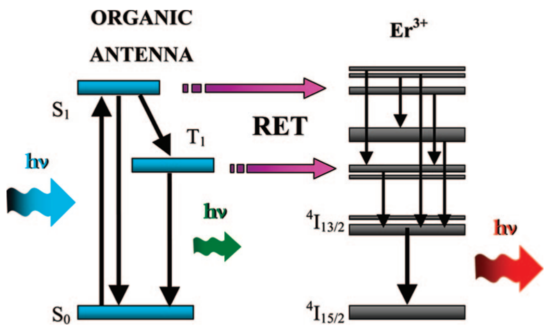

Figure 8. Jablonski diagram depicting intramolecular energy transfer (pink arrows) and light absorption and emission (black arrows) in Er^{3+} complexes. The singlet states S_1 of the ligand, optically excited by absorption of one NUV photon, decay either to the ground-state S_0 or to the triplet manifold T_1. Triplets can transfer to the lanthanide ion thanks to a resonant Dexter-type coupling, or decay to S_0. The rare-earth successively relaxes to the $^4I_{13/2}$ state, which can radiatively decay through the emission of one NIR photon at 1.54 μm.

F_7,[12] so that one should always end up with at least one CF_2H group in the coordination sphere of the final product. This residual C−H bond thus quenches very efficiently. We have taken advantage of the extreme sensitivity of the PL decay times to the nonradiative quenching processes to evaluate, by using the previously discussed model, the residual content of C−H bonds in the final material, because the ^1H and ^{19}F NMR spectra are too broad, as pointed out above. On the basis of the measured lifetime of complex **2**, we may assume that a single C−H bond in the first coordination sphere is present and corresponds to a CF_2H group in agreement with the purity of heptafluoroacetylacetone (Hacac-F_7).[12]

Ligand-Ion Energy Transfer. The kinetics of the energy transfer from the antenna to the NIR Er^{3+} emitter has been investigated. The Jablonski diagram reported in Figure 8 shows the excited-state processes occurring in the complex before NIR emission takes place. Absorption of near UV radiation directly excites the fluorinated phosphine oxide ligands, acting as antennas, to the singlet state S_1; this process is then followed by singlet−triplet conversion and resonant energy transfer from the triplet manifold T_1 of the antenna to the Er^{3+} ion. The complex can also relax back to the ground-state S_0 directly from the singlet and triplet states of the fluorinated phosphine oxide ligand. The kinetic competition between these channels of decay and the RET process for the NIR emission ($S_1 \rightarrow T_1 \rightarrow Er^{3+}$) ultimately determines the effective excitation yield of the rare-earth ion.

The photoluminescence spectrum of the complex **2** in CCl_4 solution in the spectral range between 400 and 1000 nm is shown in Figure 9. The spectrum consists of a few narrow structures on top of a broad emission, peaked in the blue and extending down to 800 nm. The wavelengths of the narrow lines coincide with the emission wavelengths from several hot levels of the Er^{3+} ion.[23] Accordingly, these structures have been assigned to the intraion transitions $^2H_{11/2} \rightarrow {}^4I_{15/2}$, $^3C_{3/2} \rightarrow {}^4I_{15/2}$, $^4F_{9/2} \rightarrow {}^4I_{15/2}$, and $^4I_{11/2} \rightarrow {}^4I_{15/2}$. The decay $S_1 \rightarrow S_0$ of the singlet of the fluorinated phosphine oxide, yields the broad peak in the blue. The low-energy

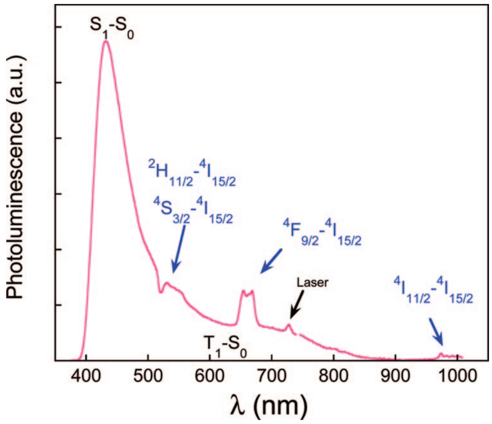

Figure 9. CW-Photoluminescence spectrum of **2** in CCl_4 solution in the spectral range 400−1000 nm (λ_{exc} = 355 nm). Narrow peaks are due to light emission from hot states of the ion. The broad peak at 430 nm is assigned to $S_1 \rightarrow S_0$ singlet recombination. $T_1 \rightarrow S_0$ radiative recombination of triplets contributes to the low energy emission of the spectrum. The short-wavelength part of the $S_1 \rightarrow S_0$ band is cut by a 400 nm spectral filter.

tail of the photoluminescence spectrum is tentatively assigned to radiative recombination of triplets.

Radiation emission related to the $T_1 \rightarrow S_0$ transition was also observed in the case of other metal complexes.[24,25] The enhancement of the triplet phosphorescence was ascribed to the presence of the rare hearth ion, which reinforces the oscillator strength of one-photon transitions between levels of different multiplicity, because of the strong spin−orbit coupling.[24] Panel A of Figure 10 shows the spectrum of the radiation emitted in two different temporal windows, 0−100 ps and 300−1500 ps, respectively. The $S_1 \rightarrow S_0$ emission disappears quickly after excitation, leaving a red-shifted spectrum characterized by a longer characteristic decay time, that we assign to $T_1 \rightarrow S_0$ and intraion transitions. Panel B of Figure 10 reports the decay of the photoluminescence signal at four wavelengths. A fast component is observed with decay time less than 10 ps. This fast contribution is spectrally peaked in the blue and, consequently, it is attributed to the decay of the S_1 population. The short lifetime of S_1 supports a very efficient spin-triplet conversion, which can be again traced back to the rare earth ion effect.[26] The photoluminescence spectrum around the transition $^4F_{9/2} \rightarrow {}^4I_{15/2}$ is reported in panel C of Figure 10 at various delays from the excitation. The intensity of the intraion emission grows up in a time-scale of ∼100 ps. This risetime is closely correlated with the contextual simultaneous decay, ∼ 70 ps, of triplets that we, thus, assign to the $T_1 \rightarrow Er^{3+}$ energy transfer process. In conclusion, we have confirmed that the fluorinated triphenyl phosphine oxide acts as an efficient antenna characterized by a fast energy transfer to the NIR Er^{3+} emitter, because of the enhanced spin-triplet conversion of S_1.

---

(23) Gordon, J.; Ballato, J.; Smith Jr, D. W.; Jin, J. *J. Opt. Soc. Am., B* **2005**, *22*, 1654–1659.

(24) Khreis, O. M.; Curry, R. J.; Somerton, M.; Gillin, W. P. *J. Appl. Phys.* **2000**, *88*, 777–780.

(25) Cölle, M.; Gärditz, G. *Appl. Phys. Lett.* **2004**, *84*, 3160–3162.

(26) Beljonne, D.; Shuai, Z.; Pourtois, G.; Bredas, J. L. *J. Phys. Chem.* **2001**, *105*, 3899–3907.

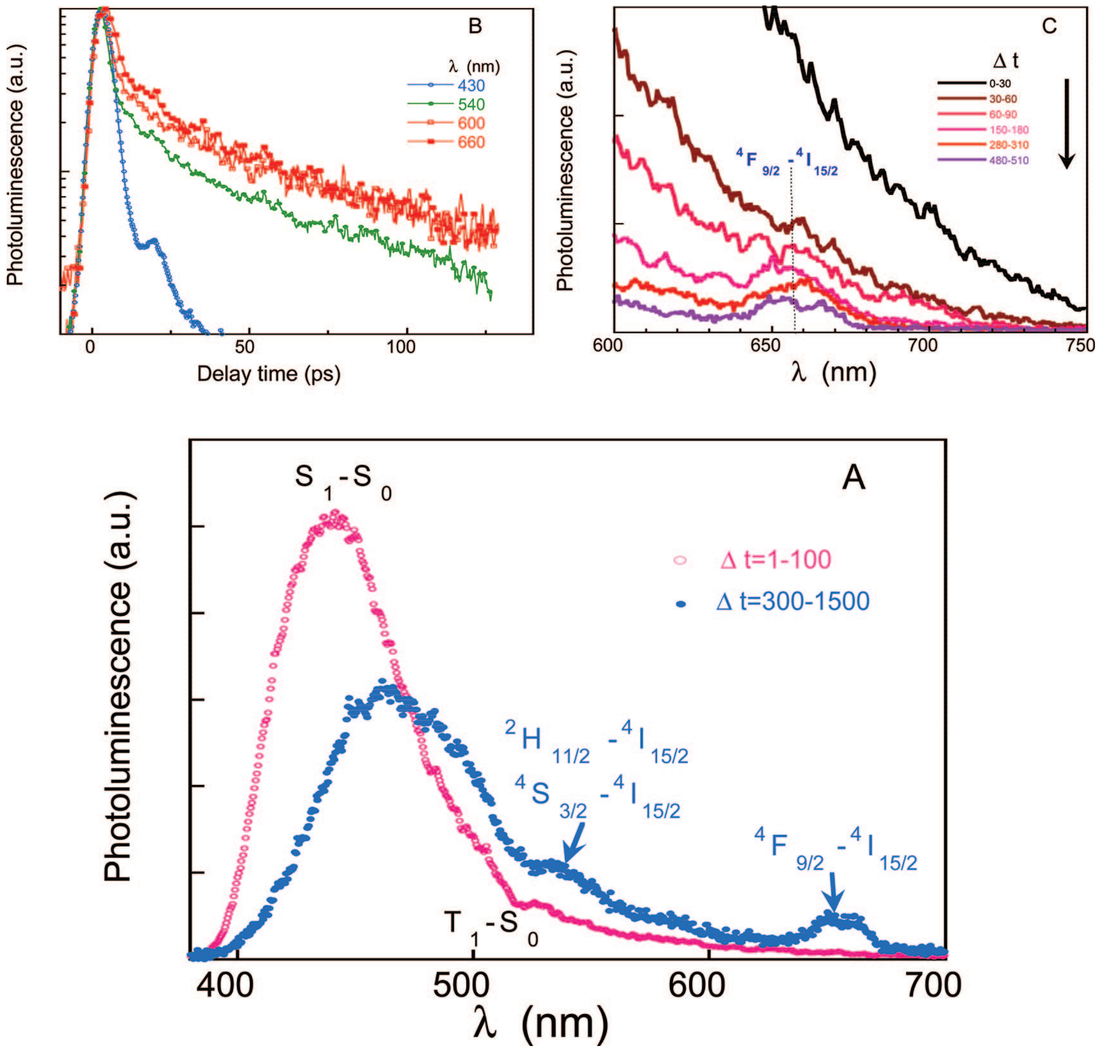

Figure 10. Time-resolved photoluminescence spectra of complex **2** in CCl_4 solution. (A) Spectra of the light emitted by **2** in the time-windows 0−100 ps and 300−1500 ps, respectively. (B) Decay of the photoluminescence signal for various wavelengths. (C) Photoluminescence spectra around the transition $^4F_{9/2} \rightarrow {}^4I_{15/2}$ at various delays from the excitation pulses.

Conclusions

Er^{3+} complexes with organic ligands can be envisaged as the active material of a new generation of solution-processed amplifiers for optical communications. Thanks to the high-absorption cross-section of organolanthanides, the planar amplifier has the potential to be optically pumped by an inorganic LED in a non critical top-geometry, thus realizing a compact, electrically driven Er-based amplifier. Recent progresses in the technology of high-power light-emitting diodes have concretized in radiant flux approaching ∼1 W and emission extended to the blue and near-ultraviolet (NUV).[27] LED output powers, however, drop drastically for wavelengths below 360 nm, setting a lower-wavelength limit to sensitization of the Er^{3+} emission in the NUV.[28]

In this paper, we have synthesized a new Er^{3+} complex partially fluorinated and another completely fluorinated, containing three partially (acac-F_6) or totally fluorinated acetylacetonates (acac-F_7) and two completely fluorinated triphenylphosphine oxides. The latter is, to our knowledge, the first octa coordinated Er^{3+} complex, based on acetylacetonates, containing totally fluorinated ligands.

Thanks to the presence of fluorinated triphenylphosphine oxide as efficient antenna, the two new complexes **1** and **2** here investigated show a lowest absorption band at 300−375 nm, peaked at 330−360 nm, perfectly matching the emission wavelength of high-power, commercial LEDs. We find that, by pumping at 355 nm, the excited state $^{4I}{}_{13/2}$ of the Er^{3+} ion in complexes **1** and **2** decays in 2.4 and 16.8 μs, respectively. The latter lifetime leads to 1 order of magnitude improvement in the NIR emission yields, compared with nonfluorinated Er^{3+} complexes with absorption band in the NUV,[8] but still too low if compared with the emission yield of Er^{3+} ions in inorganic matrixes or the estimated yield in hydrogen-free environments,[6] as recently reported for some perfluorinated Er^{3+} complexes but with absorption in the middle UV. By modeling the IR-quenching in terms of a resonance energy transfer model, the lifetime of **1** is in excellent agreement with the expected presence of one C−H bond in each acac-F_6, whereas the 16.8 μs lifetime of **2**, which for a totally fluorinated Er^{3+} complex, should fall in the millisecond time-scale,[9] provides strong indication that

---

(27) Nakamura, S. *Science* **1998**, *281*, 956–961.

(28) High-power single emitters in the blue and near ultraviolets are, for example, supplied by Philips Lumileds and Nichia Corporation.

the nominally fully fluorinated acac-F_7 ligand actually contains still a residual hydrogen content.

The present optical investigation provides the essential physical information to assess the good light harvesting properties of fluorinated phosphine oxide and the feasibility of using Er^{3+}complexes with fluorinated organic ligands in LED-pumped planar amplifiers. As the excitations in the fluorinated phosphine oxide ligands completely transfer to the Er^{3+}ion, the threshold irradiance needed to invert the ion population can be expressed as $I_{th} \approx \hbar\omega_{ex}/(\tau_{IR}\sigma_{ex})$, where $\hbar\omega_{ex}$ is the quantum energy of the exciting photons, τ_{IR} the lifetime of the excited-state of the Er^{3+}ions, and σ_{ex} is the ligand absorption cross-section. In complex **2**, σ_{ex} is 3.5×10^{-17} cm^2 at 365 nm, therefore we obtain $I_{th} \approx 1$ kW/cm^2, a value significantly higher than the maximum radiant flux ~30 W/ cm^2 delivered by a high-power LED. Nevertheless, 2 orders of magnitudes improvements could be achieved in totally perfluorinated Er^{3+} complexes of high purity, thanks to their long lifetimes of decay in the NIR region, in the range of 1−5 ms. The efficient inhibition of non radiative decay channels results in a threshold intensity downscaled to 3−15 W/cm^2, strongly encouraging us to further pursue the objective of synthesizing fully fluorinated antennas of high purity to sensitize Er^{3+}emission in the NIR.

Acknowledgment. This work was supported by Fondazione CARIPLO (2005, research title: Nuovi materiali con nanoorganizzazione di cromofori in sistemi Host−Guest o su scaffold inorganico per dispositivi fotoluminescenti o optoelettronici), FIRB-MIUR (“Synergy”), and RTN-NANOMATCH. We also thank Prof. Renato Ugo for useful discussions.

CM8024445